J. Fluid Mech. (1991), *vol.* 231, *pp.* 529–543
Printed in Great Britain

A parametric acoustic instability in premixed flames

By G. SEARBY AND D. ROCHWERGER
Laboratoire de Recherche en Combustion, URA D1117 du CNRS,
Faculté des Sciences de St Jérôme, Service 252, 13397 Marseille, Cedex 13, France

(Received 28 November 1990 and in revised form 5 April 1991)

We present an experimental and theoretical investigation of some aspects of the coupling between a premixed laminar quasi-planar flame front and acoustic standing waves in tubes. A multidimensional instability of the front arises from its interaction with the oscillating field of acceleration. This instability can be described by the Clavin–Williams laminar wrinkled flame theory in which the periodic acceleration created by the acoustic field is added to the acceleration due to gravity. As first suggested by Markstein, the resulting equation can be reduced to the Mathieu equation for a parametric oscillator. A cellular instability appears with a finite excitation threshold. This instability is responsible for the spontaneous generation of intense acoustic oscillations observed elsewhere. The value of the acoustic field at the threshold of instability and the wavelength of the cellular structures are measured experimentally for propane flames and are found to be in good agreement with the calculated values. It is also seen, both experimentally and theoretically, that for certain amplitudes of pumping, the parametric mechanism can also stabilize an initially unstable system.

1. Introduction

It has been known for a long time that flames can spontaneously produce acoustic oscillations in tubes and other enclosures (Mallard & Le Chatelier 1883). The generation of sound is a feed-back process in which the sound wave modulates the heat release from the flame and this modulation of heat release feeds energy back into the sound wave. Rayleigh's criterion (Rayleigh 1878) states that the acoustic wave will be amplified if the fluctuations in heat release and in acoustic pressure are in phase. A number of different mechanisms (see below) have been proposed to explain the modulation of combustion heat release by sound, but no clear picture has emerged of their relative importance in any particular situation.

In this paper we will be concerned with a premixed flame propagating freely in a tube closed at one end and open at the other. The acoustic modes are longitudinal with a velocity node at the closed end. This configuration has been studied experimentally by Kaskan (1953) who concludes that the coupling to the acoustic field is essentially due to variations of the flame surface area within the oscillating acoustic boundary layer close to the walls of the tube. On the other hand Markstein (1951, 1953, 1964, 1970) and Leyer (1969) have produced theoretical and experimental evidence to suggest that the coupling arises from variations in the flame area produced by oscillations of the amplitude of cellular structures subjected to the acoustic acceleration field. Dunlap (1950) has suggested that the adiabatic temperature fluctuation caused by a pressure wave will modulate the local heat

release rate of a premixed flame with the correct phase relationship. Clavin, Pelcé & He (1990) have treated this last effect in detail using a one-step high-activation energy flame. They show theoretically that the strength of this one-dimensional coupling is weak but can be sufficient, in some cases, to overcome the natural acoustic damping of a tube.

In recent experimental study of premixed propane flames in a tube, Searby (1991) has observed two different self-excited acoustic instabilities which can occur successively in time and in space for a given mixture. For moderately slow lean flames (laminar flame speed in the range 16–25 cm/s in a 1.2 metre tube) he observes a 'primary' acoustic instability that saturates in amplitude producing a flat flame. The initial growth rate of the primary instability is much higher than that expected for the one-dimensional instability of Clavin *et al.* This 'primary' instability has been studied theoretically by Pelcé & Rochwerger (1991). For faster flames Searby observes that the 'primary' instability is followed by a 'secondary' instability, with an even faster growth rate, which produces a pulsating cellular flame. This paper is mainly concerned with the interpretation of the 'secondary' instability.

The origin of the secondary instability is similar to that of the Faraday instability (Faraday 1831) observed for free liquid surfaces subjected to a periodic vertical acceleration. The pulsating cells oscillate with a period that is twice the acoustic period. This frequency halving in a flame producing acoustic oscillations was first noticed by Markstein (1953) who recognized it as being the characteristic signature of a parametrically pumped oscillator. A parametric oscillator is a resonant system which is driven by a time dependent modulation of the restoring force, or natural frequency, rather than by an external force (see Landau & Lifchitz 1966, for example). Markstein has developed an analysis based on a phenomenological model of the flame front (Markstein 1951, 1964, 1970). Leyer (1969) has studied a self-excited flame in a tube and confirms the main results of Markstein's work. This mechanism of pyro-acoustic instability seems to have been overlooked in more recent work.

The advances presented in this paper are twofold. First, we show how a theoretical description of the parametric instability can be derived rigorously using laminar flame theory developed recently. We consider only the effect of a given acoustic wave on the combustion front. The complete acoustic problem is not addressed here. It will be seen that, in general, there are two unstable branches which are identified with the 'primary' and 'secondary' instabilities mentioned above. The laminar flame model describes the effects of weak curvature exactly and allows quantitative comparison with experimental results. The details of the internal structure of the flame appear only via a single dimensionless parameter, Ma, called the Markstein number which can either be evaluated theoretically for a particular chemical scheme or measured experimentally (Searby & Quinard 1990). However volume heat losses and boundary-layer effects are not included here.

Secondly, we provide a detailed experimental study of a stationary premixed propane flame in an imposed acoustic field. This configuration is simpler than that of the transitory self-excited flame used in previous studies. Since all the parameters are controlled independently, it allows for precise measurements of the instability threshold and of the size of associated structures on the flame front which can be compared with the values predicted by the theoretical expressions.

Section 2 is devoted to the presentation of theoretical results concerning flame dynamics. In §3 we present the theory of the parametric instability, in §4 we present our experimental results and compare them with the theoretical calculations.

2. The laminar flame model

We consider an infinite quasi-planar laminar flame propagating downwards with respect to gravity and subjected to a planar acoustic field whose wave vector is normal to the average flame front and whose wavelength, Λ, is very large compared to the thickness, d, of the diffusion zone associated with the flame front. We use the results obtained for the multi-scale wrinkled flame model introduced by Clavin & Williams (1982). The original model has been extended to include the effects of hydrodynamic feedback (Pelcé & Clavin 1982). This model is valid in the limit of a high normalized activation energy, $\beta \to \infty$, and in the limit of large-scale wrinkling, $d/\lambda \to 0$, where λ is the lengthscale of wrinkling. These restrictions will be satisfied by the experimental conditions used below.

For the sake of simplicity we will use, as a starting point, the results of Searby & Clavin (1986) concerning the response of a wrinkled flame to a weakly turbulent upstream flow. Coupling reaction diffusion phenomena with hydrodynamic effects, they have obtained an equation for the local evolution of a fluctuation of the flame front position $\alpha(\boldsymbol{k}, \omega)$ in terms of an arbitrary upstream turbulent flow, $\boldsymbol{u}_e(\boldsymbol{k}, \omega)$, where $\boldsymbol{k}$ is the wavenumber of a Fourier component of wrinkling of the front and ω is the frequency (see their equation (26)):

$$[(\mathrm{i}\omega)^2 A + \mathrm{i}\omega B + C]\,\alpha(\boldsymbol{k}, \omega) = \boldsymbol{u}_e(k, \omega). \tag{1}$$

In the following, unless specified otherwise, the units of length and time are normalized by the flame thickness, d, and the flame transit time, τ, respectively, so that $\boldsymbol{k}$ is a small quantity. The values of d and τ are defined by: $d = D_{\mathrm{th}}/U_{\mathrm{L}}$, $\tau = d/U_{\mathrm{L}}$, where D_{th} is the thermal diffusivity of the fresh mixture and U_{L} is the laminar flame velocity. The coefficients A, B and C are given by:

$$\left.\begin{aligned} A &= (2-\gamma) + \gamma \boldsymbol{k}(Ma - J/\gamma), \\ B &= 2\boldsymbol{k} + \frac{2}{1-\gamma}\boldsymbol{k}^2(Ma - J), \\ C &= \frac{\gamma}{Fr}\boldsymbol{k} - \frac{\gamma}{1-\gamma}\boldsymbol{k}^2\left\{1 + \frac{1-\gamma}{Fr}\left(Ma - \frac{J}{\gamma}\right)\right\} \\ &\quad + \frac{\gamma}{1-\gamma}\boldsymbol{k}^3\left\{h_{\mathrm{b}} + (2+\gamma)\frac{Ma}{\gamma} - \frac{2J}{\gamma} + (2Pr-1)H\right\}, \end{aligned}\right\} \tag{2}$$

where $\gamma = (\rho_{\mathrm{u}} - \rho_{\mathrm{b}})/\rho_{\mathrm{u}}$ is the normalized gas expansion coefficient, ρ is the gas density, the subscripts u and b refer to the unburned and burned gases respectively. $\theta = (T - T_{\mathrm{u}})/(T_{\mathrm{b}} - T_{\mathrm{u}})$ is the normalized temperature, $h(\theta)$ is the ratio of thermal diffusivity multiplied by density at temperature θ to its value in the unburned gases, h_{b} is the value of $h(\theta)$ in the burned gases, Pr is the Prandtl number, assumed to be independent of the temperature, the inverse Froude number, Fr^{-1}, is the dimensionless acceleration gd/U_{L}^2 where g is the acceleration due to gravity,

$$H = \int_0^1 (h_{\mathrm{b}} - h(\theta))\,\mathrm{d}\theta, \quad J = \frac{\gamma}{1-\gamma}\int_0^1 \frac{h(\theta)}{1 + \theta\gamma/(1-\gamma)}\,\mathrm{d}\theta, \tag{3}$$

and Ma is the Markstein number, of order unity, which is a measure of the sensitivity of local flame velocity to curvature and stretch (see for instance Clavin 1985). For a

simplified flame model with a one-step chemical reaction, an asymptotic expansion in large values of the Zeldovich number, $\beta \gg 1$, yields the following expression for the Markstein number:

$$Ma = \frac{J}{\gamma} - \tfrac{1}{2}\beta(Le-1)\int_0^1 \frac{h(\theta)\ln(\theta)\,\mathrm{d}\theta}{1+\theta\gamma/(1-\gamma)}, \tag{4}$$

where the Zeldovich number, β, is the reduced activation energy of the reaction rate and the Lewis number, Le, is the ratio of the thermal diffusivity in the reactive mixture to the molecular diffusivity of the deficient species. Le is assumed to be constant and such that $Le-1 \approx O(1/\beta)$.

Taking the inverse time Fourier transform of (1) we obtain, in the absence of upstream turbulence ($\boldsymbol{u}_e = 0$), the following equation of motion for the flame front:

$$A\ddot{\alpha}_{tt}(\boldsymbol{k},t) + B\dot{\alpha}_t(\boldsymbol{k},t) + C\alpha(\boldsymbol{k},t) = 0, \tag{5}$$

where the dots denote time derivatives. This equation has the form of a damped harmonic oscillator. The damping, B, is always positive. The stability of the planar solution for the front depends on the sign of the coefficient C. This problem has been discussed by Pelcé & Clavin (1982). The sign of C depends on the values of the Froude number, the wavenumber of the wrinkling and on the diffusive properties of the mixture. However, except for very slow downward propagating flames, C is always negative for some range of wavenumbers, implying that the planar front is unstable. The physical origin of the instability is hydrodynamic, as first described by Darrieus (1938) and by Landau (1945).

In the problem considered here, the flame front is periodically displaced by a planar sound wave. The front is invariant by translation but the Froude number in (2) must be replaced by a term containing the total dimensionless acceleration experienced by the front:

$$\frac{gd}{U_L^2} - \omega_a u_a \cos(\omega_a t),$$

where ω_a is the dimensionless acoustic frequency and u_a is the dimensionless acoustic velocity at the front. Separating the coefficient C into a constant part C_0 and a time dependent part C_1, (5) becomes:

$$A\ddot{\alpha}_{tt}(\boldsymbol{k},t) + B\dot{\alpha}_t(\boldsymbol{k},t) + [C_0 - C_1\cos(\omega_a t)]\,\alpha(\boldsymbol{k},t) = 0, \tag{6}$$

with

$$C_1 = \gamma k \omega_a u_a \left\{1 - k\left(Ma - \frac{J}{\gamma}\right)\right\}, \tag{7}$$

equation (6) is now in the form of a parametrically driven damped harmonic oscillator, with coefficients which depend on the wavelength of wrinkling of the front. A phenomenological equation of the same form as (6) has been proposed previously by Markstein (1951). The contribution of the development described above is to give theoretical expressions for the coefficients A, B and C which are obtained from a rigorous analysis of the flame structure. It is important for the following to stress that Ma is the only parameter whose theoretical expression is sensitive to the details of the internal structure of the flame, represented by Le and β in the simple model. All the other coefficients can be obtained from knowledge of the flame temperature and the thermodynamic properties of the gases independently of the detailed transport properties and chemical kinetics of the reactive mixture. In contrast with kinetic properties, parameters such as the gas expansion coefficient, γ, are easily

measured. Thus the theoretical expressions (2) provide a convenient framework for an experimental comparison with (6) in which Ma can be treated as the only free parameter.

3. The parametric oscillator

Following Markstein (1964) we make the following substitutions:

$$\left.\begin{aligned} z &= \tfrac{1}{2}\omega_a t, \quad \kappa = \frac{B}{\omega_a A}, \\ a &= \frac{4AC_0 - B^2}{\omega_a^2 A^2}, \quad q = \frac{2C_1}{\omega_a^2 A}, \\ \alpha &= Y(z)\,\mathrm{e}^{-\kappa z}\,\mathrm{e}^{\mathrm{i}ky}. \end{aligned}\right\} \tag{8}$$

With these substitutions, (6) reduces to the well-known Mathieu equation:

$$Y'' + [a - 2q\cos(2z)]\,Y = 0, \tag{9}$$

where the primes now denote differentiation with respect to z. The Mathieu equation is similar to that of the harmonic oscillator, but with a restoring force that is a periodic function of time. The solutions, $Y(z)$ of (9) may be written in the form (McLachlan 1951)

$$Y(z) = A_1 \exp(\mu z)\,\phi(z) + A_2 \exp(-\mu z)\,\phi(-z), \tag{10}$$

where $A_{1,2}$ are two arbitrary constants, $\phi(z)$ is a function that is periodic with period π or 2π, and $\mu(a, q)$ is either real or imaginary, corresponding to unstable or stable solutions respectively. From the change of variables in (8) it can be seen that the condition of marginal stability for the flame is given by $\mu = \kappa$. For given values of a (natural frequency squared) and q (amplitude of excitation), the corresponding value of μ may be determined numerically by the continued fraction method (see for instance Abramowitz & Stegun 1972). It must be remembered that a is a function of the wavenumber, $\boldsymbol{k}$, so that the flame has no unique resonant frequency but a continuum of frequencies associated with a continuum of possible wavelengths of structures on the front.

The standard variables a, q and μ do not form a convenient set for representing the dynamic properties of a flame front. We will choose instead to present the results in terms of the physical dimensionless variables ω_a, u_a, $\boldsymbol{k}$, Ma and Fr.

Figure 1 shows typical stability diagrams presented in the $u_a, \boldsymbol{k}$ plane for various values of the reduced frequency, the Markstein number and the Froude number. The vertical coordinate should be thought of as the reduced acceleration $(\omega_a U_a)/(\omega_a U_L)$, which is the physical parameter driving the instability. The numerical values used in figure 1 (a) for the various parameters are representative of the flames presented in our experimental study.

As already noticed by Markstein (1964), there are two distinct unstable regions, labelled I and II. The lower region extends down to zero amplitude of acoustic excitation where it corresponds to the well-known Darrieus–Landau planar flame instability. It is stabilized at large wavenumbers by diffusive effects and at very small wavenumbers by the effect of gravity. In this domain the cellular structures on the front oscillate at the acoustic frequency. We identify these oscillations of flame area in this lower unstable region as the mechanism leading to the 'primary' acoustic

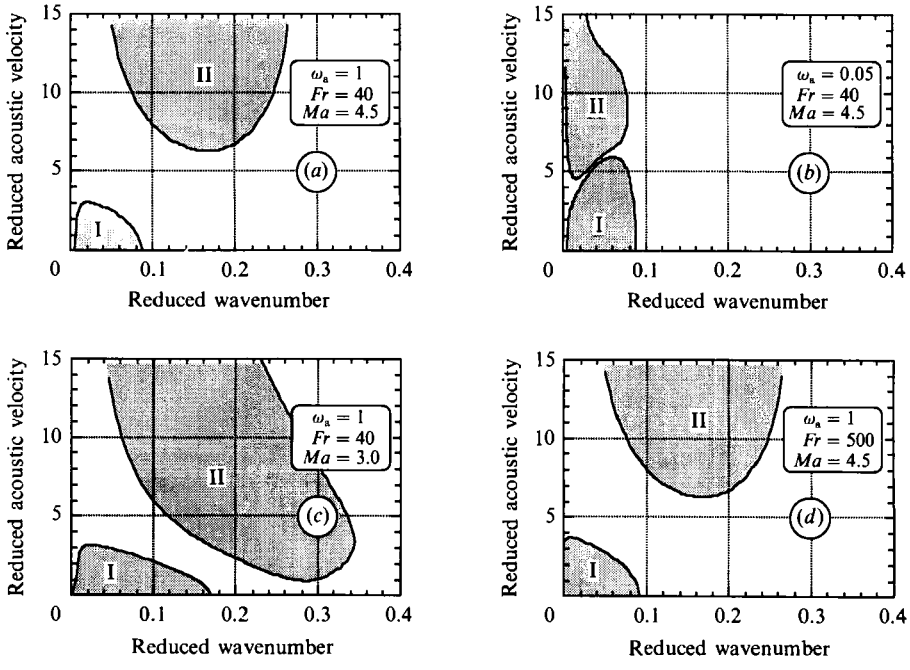

FIGURE 1. Stability diagrams for parametrically excited flames in the plane of reduced acoustic velocity, $u_a = U_a/U_L$, and reduced wavenumber, $k = 2\pi d/\lambda$. (*a*) The values of the dimensionless quantities are: $\omega_a = 1.0$, $Fr = 40$ and $Ma = 4.5$. These values correspond to a laminar flame speed of 20 cm/s and a real frequency of 304 Hz. (*b*) Effect of changing the reduced frequency: $\omega_a = 0.05$, $Fr = 40$ and $Ma = 4.5$. These values correspond to a laminar flame speed of 20 cm/s and a real frequency of 15 Hz. (*c*) Effect of changing the Markstein number: $\omega_a = 1.0$, $Fr = 40$ and $Ma = 3.0$. (Same flame speed and frequency as in (*a*.) (*d*) Effect of changing the Froude number: $\omega_a = 1.0$, $Fr = 500$ and $Ma = 4.5$. These values correspond to a laminar flame speed of 47 cm/s and a real frequency of 1639 Hz. The other parameters have values appropriate for a lean propane flame.

instability of Searby (1991). A theoretical description of this phenomenon has been recently developed by Pelcé & Rochwerger (1991). A remarkable feature is that the Darrieus–Landau instability can be *re-stabilized* by the oscillating acoustic acceleration and in general there exists a range of reduced acoustic velocities in which the planar flame is stable. In figure 1 (*a*) the re-stabilization occurs when the local acoustic velocity is about 3.2 times the laminar flame velocity and ends when the acoustic velocity reaches about 6.3 times the laminar flame velocity.

In the upper unstable domain the structures on the flame oscillate at half the acoustic frequency, it is the domain of parametric instability. The fact that a finite value of excitation is needed to excite this instability is directly related to the presence of a damping term in the original equation of evolution (6). We identify the oscillations of flame area in this upper unstable region as the mechanism leading to the 'secondary' acoustic instability of Searby. The effects of the non-dimensional parameters ω_a, Ma and Fr on the extent of the domains of instability are shown in figures 1 (*b*), 1 (*c*) and 1 (*d*) respectively.

Decreasing the reduced frequency, ω_a (decreasing real frequency or increasing flame velocity), causes both regions to move towards smaller reduced wavenumbers. It also lowers the threshold of the upper region and causes the upper limit of the lower region to move upwards. For sufficiently small ω_a the two regions can co-exist for some range of acoustic velocities and the planar flame is never stable because for

any reduced acoustic velocity there is always some unstable wavelength, as shown in figure 1(*b*). For mathematical reasons the two unstable domains can never merge, but may become infinitely close. This type of stability diagram applies to propane flames close to stoichiometry at frequencies below about 100 Hz.

Decreasing the Markstein number causes both unstable regions to extend towards larger wavenumbers and also lowers the threshold of the upper region. Again, at a given frequency, the two regions overlap for values of the Markstein number below some critical value, as shown in figure 1(*c*), and the planar flame is never stable. This type of stability diagram corresponds to rich hydrocarbon flames and to lean hydrogen flames.

Increasing the Froude number (increasing flame speed at constant ω_a) has almost no effect on the upper unstable region and little effect on the lower region provided that $Fr \geqslant 20$ (flame velocity $\geqslant 15$ cm/s), see figure 1(*d*). For values of the Froude number below about 20, the lower region becomes sensitive to Fr and shrinks towards the $u_a = 0$ axis as Fr decreases. It disappears completely for sufficiently small values of Fr for which the coefficient C in (2) is always positive (not shown in figure 1). The upper region is relatively insensitive to Fr except at very small reduced frequency. This lack of sensitivity of the upper threshold to Fr will be used in the experimental section to enable the results to be presented as a function of a single parameter, ω_a.

4. Experiments

We have made an experimental study of the threshold of excitation of the upper region, II, in an imposed acoustic field. This type of experiment has not been reported previously in the literature. We used the apparatus shown in figure 2. This is a steady state experiment in which a freely propagating flame is kept stationary in the laboratory frame and interacts with a standing acoustic field generated by a loudspeaker. Previous experiments have used either transitory or anchored flames.

The walls of the burner were uncooled Pyrex glass tubes of various lengths and diameters. Premixed propane–air mixtures were fed into the bottom of the burner and traversed a 20 μm porous plate which killed turbulence and imposed a quasi top-hat velocity profile in the burner. The flame was kept stationary by manually adjusting the gas flow rate to exactly equal the mass consumption rate of the flame. Once stabilized, the heat released by the flame creates an abrupt longitudinal temperature gradient in the burner walls at the position of the flame front. This temperature gradient was then sufficient to stabilize the flame position with respect to small misadjustments of the gas flow rate. Because of the non-zero thermal conductivity of the Pyrex glass, this region of temperature gradient propagated upstream at about 0.5 mm/s carrying the flame front with it. This slow propagation could be eliminated by selectively cooling the burner ahead of the flame position, but this precaution proved to be superfluous in these experiments since only a few minutes were required to perform each series of measurements. Cooling the downstream walls of the burner causes strong thermal convection cells to form behind the flame, disrupting the top-hat velocity profile and perturbing the dynamics of the flame. Downstream cooling was not used here.

The tube was excited acoustically at one of its resonant frequencies by a loudspeaker mounted just below the porous plate. The burner was excited in either the $\frac{1}{4}$ wavelength or the $\frac{3}{4}$ wavelength longitudinal mode. In these modes there is a velocity node at the closed end of the burner and a pressure node in the vicinity of

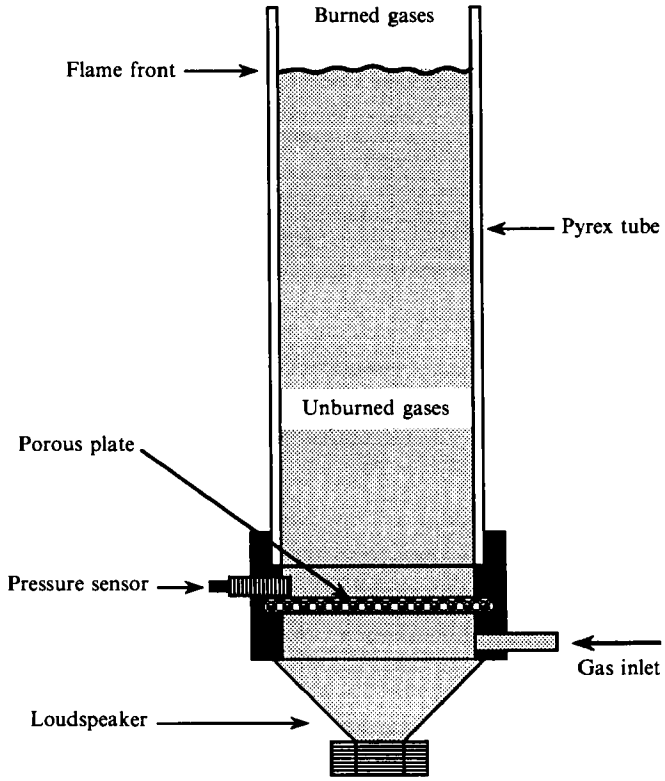

FIGURE 2. Diagram of the experimental apparatus. Tube lengths were 50–150 cm with diameters of 6 and 10 cm. The flame front was held at constant height by adjusting the mixture flow velocity.

the open end. The pressure fields in the cold tubes were investigated with a small microphone and it was found that, at resonance, the pressure antinode was always situated within 1 or 2 mm of the porous plate. The presence of the flame changes the resonant frequency of the tube because of the increased sound velocity in the burned gases and the phase jump at the density interface associated with the flame, however the lower pressure antinode remains attached to the porous plate. A piezoelectric pressure sensor, placed adjacent to the porous plate, was used to measure the acoustic pressure level in the experiments with flames. Knowing the acoustic pressure at the bottom of the burner and the frequency of the standing wave, the phase and acoustic velocity at the flame front is easily calculated.

The flame front was maintained approximately one diameter from the burner exit. The flames were thus situated close to a pressure node, so that energy feedback into the acoustic wave was small and spontaneous acoustic oscillations were not observed. In a typical experiment, the acoustic level was adjusted to produce a stable planar flame and the flame was positioned one diameter from the open end of the tube. Extremely flat flames could be obtained in this way, see figure 3. The frequency of excitation was re-adjusted to exact resonance and the acoustic level was slowly increased until the threshold, u_a^*, was reached and structures appeared at a finite wavenumber $\boldsymbol{k}^*$, see figure 1(*a*). This experiment was repeated for different equivalence ratios and for different acoustic frequencies. The structures appeared abruptly, and for a single experiment, the level of threshold could be determined to within 1 %, however, the thermal gradients just ahead of the flame front produced

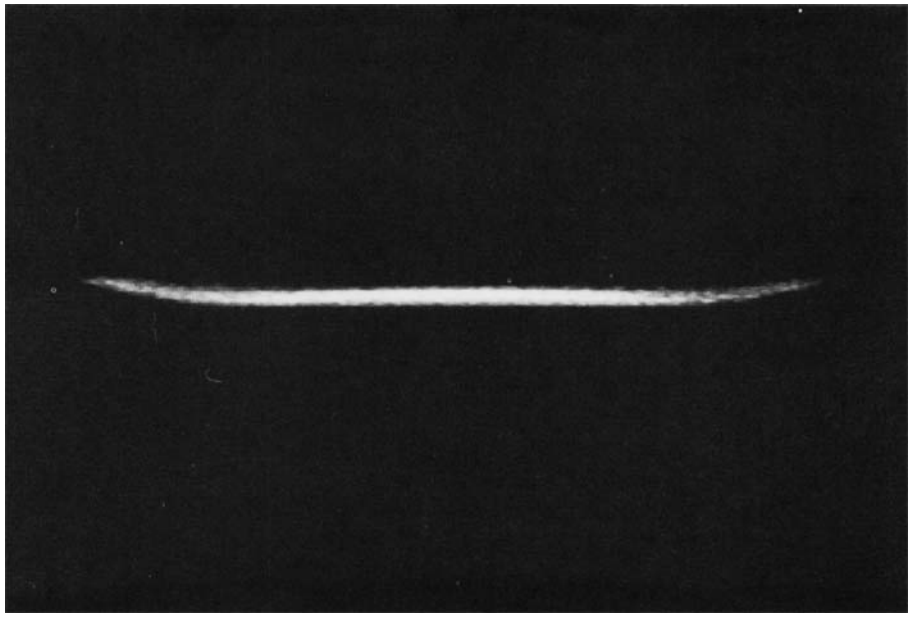

FIGURE 3. Side-on photograph of a planar propane–air flame stabilized by the presence of an acoustic field, just below the threshold of parametric instability. Equivalence ratio = 0.585, $\omega_a = 0.58$, $Fr = 10.6$.

slight deviations from the top-hat velocity profile and the associated velocity gradients caused experiment-to-experiment variations of up to 5%.

The experiments were limited to the range of conditions for which the planar flame can exist, i.e. for flames whose two domains of instability are well separated as in figures 1(*a*) or 1(*d*). We have chosen to work with sufficiently lead propane air mixtures because it is known that the Markstein number of these flames is nearly constant and has an experimentally measured value of 4.5 ± 0.5 (Searby & Quinard 1990). For this value of the Markstein number and for the frequencies used in the experiments, this condition poses an upper limit of roughly 20 cm/s on the flame velocity. The minimum value of flame velocity was limited only by the weak extinction limit at approximately 7.2 cm/s. For propane–air flames close to stoichiometry the stability diagram is of the type shown in figure 1(*b*) and the planar flame is never stable for any acoustic intensity. For rich propane–air mixtures the Markstein number is known to be much smaller and the stability diagram is of the type shown in figure 1(*c*), again with no region of stability for the planar flame. In the light of the above considerations the propane–air flames were restricted to equivalence ratios in the range $0.5 < \Phi < 0.7$.

The experiments were carried out with tubes of various lengths (150, 100 and 50 cm) and two diameters, 10 cm and 6 cm. The frequency of excitation was varied from 57 Hz (150 cm tube, fundamental mode) to 265 Hz (100 cm tube, first harmonic). The 50 cm tube was not used at its harmonic frequency because the acoustic losses were too great. The instability threshold was reached with power levels of a few watts at the loudspeaker. Typical acoustic velocities at the flame were of the order of 1 m/s and the corresponding acoustic accelerations were of the order of 500 m/s^2. Changing the diameter of the tube produced no significant change to the thresholds indicating that boundary effects, such as those invoked by Kaskan, were not dominant.

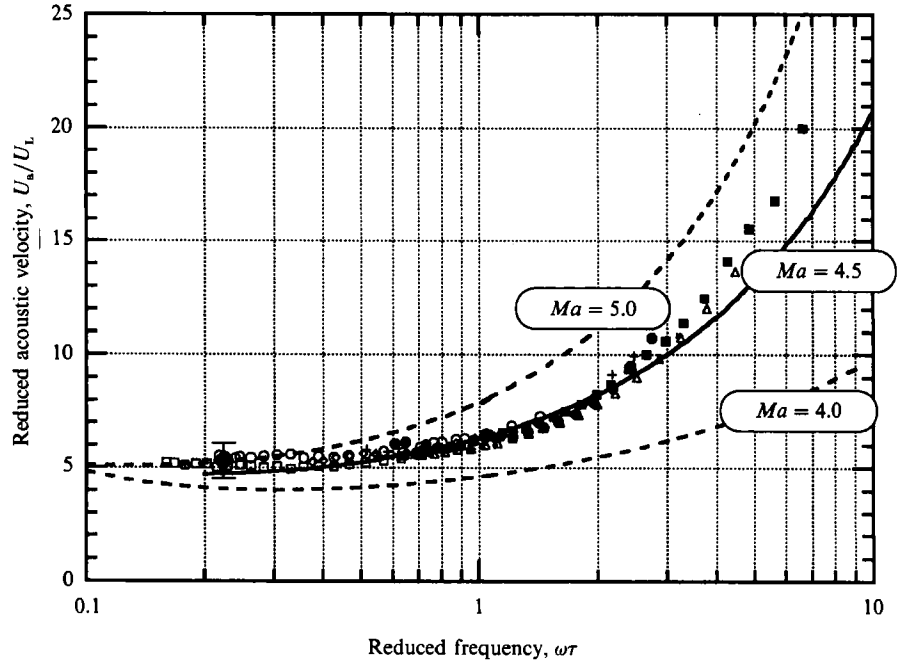

FIGURE 4. Experimental determination of the threshold of parametric instability in reduced coordinates ω_a and u_a. The points represent 160 independent measurements on flames of different speeds at different acoustic frequencies in tubes of different lengths and diameters. We also show the calculated value for the threshold. ——, Ma = 4.5; – – –, Ma = 4.0, 5.0. ◆, threshold obtained from Searby (1991), his figure 4(*b*).

	Dimensioned constants
$g = 981$ cm/s^2	Acceleration due to gravity
$D_{th} = 0.22$ cm^2/s	Thermal diffusivity in unburned gas
	Dimensionless constants
$Pr = 0.689$	Prandtl number
$\gamma = 0.822$	Normalized gas expansion factor
$h_b = 3.19$	Normalized gas diffusivity
$H = 0.96$	
$J = 3.33$	
	Dimensioned variables
$d = D_{th}/U_L$	Flame thickness
$\tau = D_{th}/U_L^2$	Flame transit time
	Dimensionless variables
$\omega_a = \Omega_a \tau$	Frequency of excitation
$u_a = U_a/U_L$	Amplitude of excitation
$k = 2\pi d/\lambda$	Wave number of structures on front
$Fr = U_L^2/gd$	Froude number
Ma	Markstein number

TABLE 1. Numerical values used in calculations

The experimental results for the threshold of parametric instability are plotted in figure 4. All the results have been plotted in the reduced variables ω_a and u_a. The reduced frequency was varied both by changing the frequency of excitation and by changing the flame velocity. It can be seen that in this representation the results of

160 different measurements collapsed onto a single curve, within experimental errors. The solid and dotted lines in figure 4 represent calculated values of the threshold, for three different values of Ma, using the analysis presented in §3. These curves are the locus of the minimum of the domain of parametric instability of which one point is shown in figure 1(*a*). The calculated position of this minimum is essentially a function of the reduced frequency ω_a and of the Markstein number, Ma. It is also a function of the other mixture dependent properties such as Fr, γ, h_b, J, H. However, although the flame speed varies considerably (from about 7–20 cm/s in these experiments) the quantities γ, h_b, J, H, are only slow functions of the burnt gas temperature and in fact do not vary very much over the range of mixtures used here ($0.5 < \Phi < 0.7$). For example γ varies from 0.80 to 0.839. We have evaluated them for adiabatic combustion at an average equivalence ratio of $\Phi = 0.6$ and, for simplicity, we have assumed them to be constant, thus permitting the theoretical results to be presented as a function of only a small number of parameters. The numerical values we have used are given in table 1.

The Froude number, Fr, varies very rapidly with the flame speed, so ω_a and Fr are indeed independent parameters. However, at high flame speeds, $1/Fr$ is a very small number and can be neglected, at low flame speeds $1/Fr$ is not a small number and the extent of the lower domain of instability depends strongly on the value of Fr. Nevertheless, for the frequencies used here, the position of the minimum of the upper domain varies only slightly (less than 4%) when $1/Fr$ is varied from infinity to zero (see figures 1(*a*) and 1(*d*)). Since the experimental errors exceed 4%, we have set $1/Fr = 0$ for the purposes of calculating the thresholds in figure 4, allowing the theoretical results to be plotted as a function of only two independent variables, ω_a, and Ma.

Searby & Quinard (1990) have experimentally measured the value of the Markstein number for a number of fuels. For lean propane–air mixtures they find that $Ma = 4.5 \pm 0.5$ with negligible variation for equivalence ratios between $\Phi = 0.5$ and $\Phi = 0.9$. This finding is quite compatible with the theoretical expression for Ma, given by (4), and based on a very simple flame model which was, *a priori*, not expected to be quantitatively good for a real fuel. The solid line in figure 4 was calculated using the value $Ma = 4.5$ along with the values given in table 1. It can be seen that the experimental points closely match the calculated thresholds. For comparison we have also shown the calculated thresholds for mixtures with Markstein numbers $Ma = 4.0$ and $Ma = 5.0$. These curves show that the instability threshold is quite sensitive to the Markstein number and in fact measurements of this type may be used as a means of determining Ma.

We have also investigated the size of the structures which appear at the instability threshold. Figure 5(*a*) shows a photograph of the flame front just after the threshold, taken at an instant when the cellular amplitude is maximal. The structure is fairly regular, but the spatial correlation of orientation is low. The average cell spacing was obtained from these photographs by taking the two-dimensional Fourier transform as shown in figure 5(*b*). In this figure the signal-to-noise ratio has been improved by averaging the transforms of five independent images. The circle of wave vectors is well defined showing that the cell spacing is nearly constant, but with a random orientation in space. In figure 6 we show the results obtained for flame speeds between 8 cm/s and 20 cm/s at excitation frequencies of 57, 102 and 175 Hz. The results are plotted in the reduced coordinates, ω_a and $\boldsymbol{k}$, again it can be seen that the twelve experimental results collapse onto a single curve. The vertical error bars represent one Fourier component in the wavenumber space of figure 5(*b*). The solid

(a)

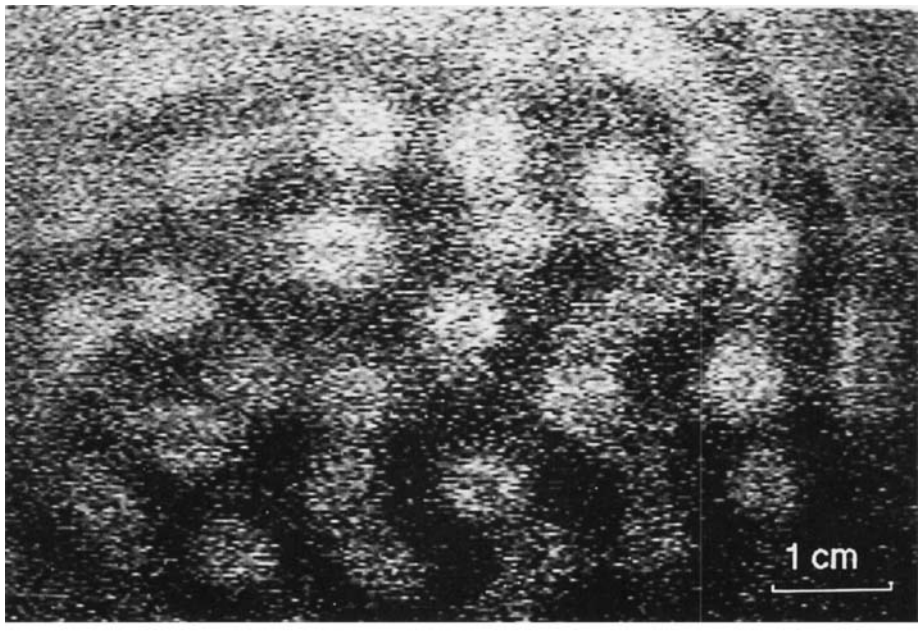

(b)

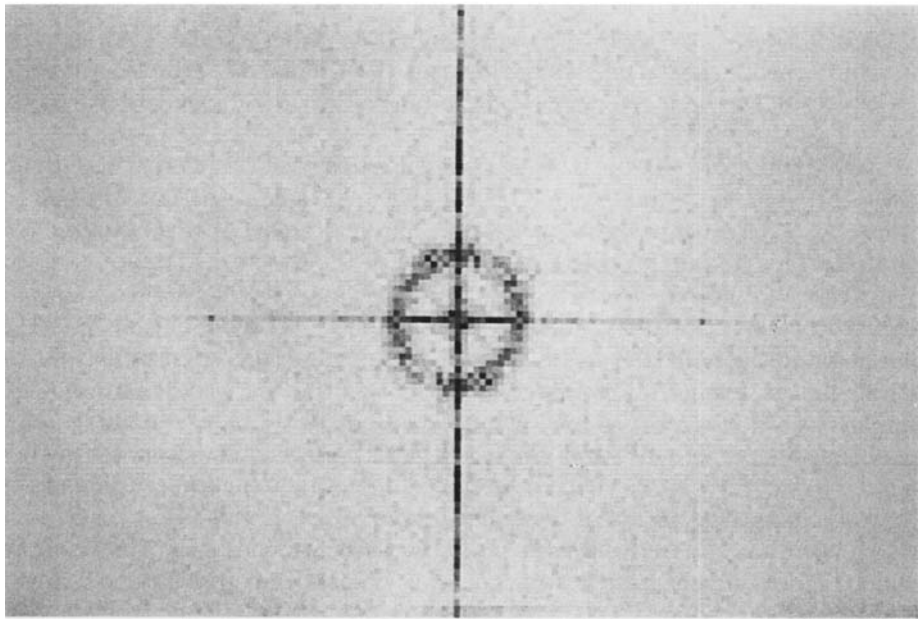

FIGURE 5. (a) Head-on photograph of acoustically excited structures on flame front. Equivalence ratio = 0.573, $\omega_a = 0.528$, $Fr = 8.5$. The average size of the structures is 1.1 cm. (b) Averaged two-dimensional Fourier transform of images including figure 5(a).

line represents the locus of $\boldsymbol{k}^*$ in figure 1(a) as a function of reduced frequency, calculated from (2) and (6) with the numerical values given in table 1 and with $Ma = 4.5$. The calculated response of the flame is again in close agreement with the experimentally measured values.

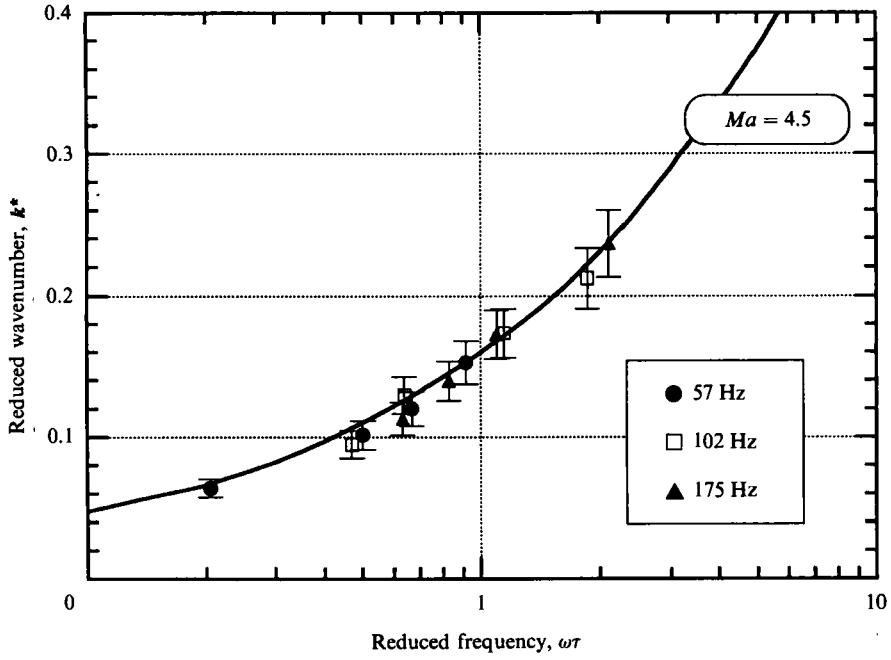

FIGURE 6. Experimental determinations of the reduced wavenumber, k^*, of the acoustically excited structures at threshold, as a function of the reduced frequency, ω_a. We also show the calculated value, solid line, evaluated with $Ma = 4.5$.

5. Conclusions

Using recent laminar flame theory, we have given a theoretical and experimental study of a parametric acoustic instability of planar flames, first recognized by Markstein (1953). The physical mechanism driving this instability is the periodic acceleration of the interface (flame) separating two regions of different density. An acoustic field of moderate intensity can first *stabilize* the natural Darrieus–Landau instability of premixed flames and then, at a higher intensity, produce a parametric cellular instability with a well-defined threshold and associated with a well-defined critical wavenumber.

Our experimental observations on lean, well controlled propane–air flames stabilized dynamically in an imposed acoustic field confirm all these points. We have measured the thresholds and critical wavenumbers. Such lean premixed propane air flames with an equivalence ratio between 0.5 and 0.9 are known experimentally to have an almost constant Markstein number, $Ma = 4.5$ (Searby & Quinard 1990). The other properties of the mixture are well known (see table 1) so that there are no adjustable parameters for the comparison between experimental and theoretical results. The calculated results are in remarkably good quantitative agreement with the experimental observations, indicating that the laminar flame theory presented in §§2 and 3 is providing a good quantitative description of the dynamics of flame fronts including acceleration effects. In the light of the sensitivity of the theoretical results to variations of Ma, our work provides, as a byproduct, a general method which may be used as a tool to measure the Markstein number of other flames.

Finally, the instability threshold observed with an imposed acoustic field may be compared with that observed by Searby (1991) in the case of self-excited acoustic oscillations of a transitory flame propagating freely in a tube. From his figure 4(*b*) it

can be seen that when the secondary instability is triggered, the acoustic pressure at the bottom of the tube is 700 Pa and the flame is 0.49 m from the bottom. The acoustic frequency is 122 Hz so the acoustic velocity at the flame, U_a, is easily calculated to be 1.45 m/s. The flame velocity is 27.5 cm/s giving $u_a = 5.3$ and $\omega_a = 0.22$. This data point is indicated in our figure 4. It lies close to our experimental points, indicating that the mechanism responsible for his self-excited secondary instability is indeed the parametric instability described here and also that the complete feedback mechanism, including acoustic losses, has little effect on the absolute threshold. It remains to be shown that this parametric mechanism can explain the very high growth rate observed in such self-excited instabilities.

We are grateful to P. Clavin and to P. Pelcé for their suggestions and enlightening discussions and to R. Miorcec de Kerdanet for his help with the experiments. This work was carried out in partial fulfilment of a contract DRET no. 88-210.

REFERENCES

ABRAMOWITZ, M. & STEGUN, I. 1972 *Handbook of Mathematical functions*, 9th edn. Dover.

CLAVIN, P. 1985 Dynamic behavior of premixed flame fronts in laminar and turbulent flows. *Prog. Energy Combust. Sci.* **11**, 1–59.

CLAVIN, P., PELCÉ, P. & HE, L. 1990 One-dimensional vibratory instability of planar flames propagating in tubes. *J. Fluid Mech.* **216**, 299–322.

CLAVIN, P. & WILLIAMS, F. A. 1982 Effects of molecular diffusion and of thermal expansion on the structure and dynamics of premixed flames in turbulent flows of large scale and low intensity. *J. Fluid Mech.* **116**, 251–282.

DARRIEUS, G. 1938 Propagation d'un front de flamme. Unpublished work presented at La Technique Moderns (1938), and at Le Congrès de Mécanique Appliquée (1945).

DUNLAP, R. A. 1950 Resonance of flames in a parallel-walled combustion chamber. *Rep. UMN-43. Aeronautical Research Center. University of Michigan, Project MX833.*

FARADAY, M. 1831 On the forms and states assumed by fluids in contact with vibrating elastic surfaces. *Phil. Trans. R. Soc. Lond.* **121**, 319–340.

KASKAN, W. E. 1953 An investigation of vibrating flames. *Fourth Symp. on Combustion*, pp. 575–591. Baltimore: Williams and Wilkins.

LANDAU, L. 1945 On the theory of slow combustion. *Acta Physicochimica URSS* **19**, 77–85.

LANDAU, L. & LIFSHITZ, E. 1966 *Mécanique* (trans. from Russian). MIR Moscow.

LEYER, J. C. 1969 Interaction between combustion and gas motion in the case of flames propagating in tubes. *Astron. Acta* **14**, 445–451.

MCLACHLAN, N. W. 1951 *Theory and Application of Mathieu functions.* Clarendon.

MALLARD, E. E. & LE CHATELIER, H. 1883 Recherches expérimentales et théoriques sur la combustion des mélanges gazeux explosifs. *Annls. Mines, Paris*, Partie Scientifique et Technique, Ser. 8, no. 4, 274.

MARKSTEIN, G. H. 1951 *J. Aero Sci.* **18**, 428.

MARKSTEIN, G. H. 1953 Instability phenomena in combustion waves. *Fourth Symp. on Combustion*, pp. 44–59. Baltimore: Williams and Wilkins.

MARKSTEIN, G. H. 1964 *Nonsteady Flame Propagation.* Pergamon.

MARKSTEIN, G. H. 1970 Flames as amplifiers of fluid mechanical disturbances. *Proc. Sixth National Congress of Appl. Mech.*, pp. 11–33. Cambridge, Mass.

PELCÉ, P. & CLAVIN, P. 1982 Influence of hydrodynamics and diffusion upon the stability limits of laminar premixed flames. *J. Fluid Mech.* **124**, 219–237.

PELCÉ, P. & ROCHWERGER, D. 1991 Vibratory instability of cellular flames propagating in tubes. *J. Fluid Mech.* (submitted).

RAYLEIGH, LORD 1878 *Nature* **18**, 319.

SEARBY, G. 1991 Acoustic instability in premixed flames. *Combust. Sci. Tech.* (to appear).

SEARBY, G. & CLAVIN, P. 1986 Weakly turbulent wrinkled flames in premixed gases. *Combust. Sci. Tech.* **46**, 167–193.

SEARBY, G. & QUINARD, J. 1990 Direct and indirect measurements of Markstein numbers of premixed flames. *Combust. Flame* **82**, 298–311.